NeuroImage 260 (2022) 119449

Contents lists available at ScienceDirect

NeuroImage

journal homepage: www.elsevier.com/locate/neuroimage

Alpha power during task performance predicts individual language comprehension

P. Wang[a], Y. He[c], B. Maess[a], J. Yue[e], L. Chen[b,f], J. Brauer[b,d], A.D. Friederici[b], T.R. Knösche[a,*]

[a] Max Planck Institute for Human Cognitive and Brain Sciences, Brain Networks Group, Leipzig, Germany
[b] Max Planck Institute for Human Cognitive and Brain Sciences, Department of Neuropsychology, Leipzig, Germany
[c] Philipps University Marburg, Department of Psychiatry and Psychotherapy, Marburg, Germany
[d] Friedrich Schiller University, Office of the Vice-President for Young Researchers, Jena, Germany
[e] Harbin Institute of Technology, Laboratory for Cognitive and Social Neuroscience, School of Management, Harbin, China
[f] Beijing Normal University, College of Chinese Language and Culture, Beijing, China

ARTICLE INFO

Keywords:
Individual alpha
Alpha attenuation
EEG/MEG
Sentence comprehension
Embedded sentences

ABSTRACT

Alpha power attenuation during cognitive task performing has been suggested to reflect a process of release of inhibition, increase of excitability, and thereby benefit the improvement of performance. Here, we hypothesized that changes in individual alpha power during the execution of a complex language comprehension task may correlate with the individual performance in that task. We tested this using magnetoencephalography (MEG) recorded during comprehension of German sentences of different syntactic complexity.

Results showed that neither the frequency nor the power of the spontaneous oscillatory activity at rest were associated with the individual performance. However, during the execution of a sentences processing task, the individual alpha power attenuation did correlate with individual language comprehension performance. Source reconstruction localized these effects in left temporal-parietal brain regions known to be associated with language processing and their right-hemisphere homologues.

Our results support the notion that in-task attenuation of individual alpha power is related to the essential mechanisms of the underlying cognitive processes, rather than merely to general phenomena like attention or vigilance.

1. Introduction

The alpha band (8–12 Hz) typically forms the most stable and prominent peak in the EEG/MEG power spectrum (Berger, 1938; Schomer and Da Silva, 2012). These oscillations evidently play a major role in brain function at rest, as their power is changed, mostly attenuated, in the task-relevant brain regions during various movement or cognitive tasks, including finger tapping, driving, arithmetic calculations, and sentence comprehension (Gastaldon et al., 2020; Klimesch et al., 1990; Kuhnke et al., 2017; Magosso et al., 2019; Mann et al., 1996; Meyer et al., 2013; Pfurtscheller, 1989; Van Schijndel et al., 2015; Vassileiou et al., 2018; Wang et al., 2021). The power attenuation in the alpha band has also been shown to scale with task demand or engagement at the group level (Magosso et al., 2019; Wang et al., 2021). This phenomenon has been associated with cortical activation or release from inhibition due to the task (Klimesch, 2012; Meyer, 2018; Pfurtscheller, 2003). It has also been shown, at the individual level, that the alpha power at rest or immediately before the task correlates with task performance (Jones et al., 2010; Van Dijk et al., 2008; van Ede et al., 2012), but evidence for such an individual relationship for the task-related power attenuation during task performance is scarce (Hilla et al., 2020). Therefore, the question remains whether the attenuation phenomenon is directly related to the essential mechanisms of the underlying cognitive processes, rather than merely to general phenomena like attention or vigilance that might be also present during resting periods in the same experiment.

In order to contribute to the clarification of this question, we turn to the arguably most 'human-like' cognitive faculty, namely language. The ability to produce and understand language requires intense coordination of numerous cognition faculties, such as phonological perception, syntax processing, semantic association, working memory, attention, and motor control. It has already been shown that the alpha band power at rest is related to individual language abilities (Kwok et al., 2019). Specifically, larger alpha band power differences between eye-open and eye-close conditions was shown to be associated to lower language scores in young children.. Moreover, we have recently explored the alpha band power *during* a language training task with center-

* Corresponding author.
E-mail address: knoesche@cbs.mpg.de (T.R. Knösche).

https://doi.org/10.1016/j.neuroimage.2022.119449.
Received 24 October 2021; Received in revised form 15 June 2022; Accepted 3 July 2022
Available online 12 July 2022.

embedded German sentences at the group level (Wang et al., 2021), and found training-related alpha power attenuation. Moreover, we also found that the cortical (posterior superior temporal and adjacent parietal) alpha band power attenuation at the final embedding closure was significantly larger for double than for single embedded sentences. However, we do not yet know if the individual alpha power during task performance is predictive of the individual cognitive performance.

In the present paper, we used the same data as in the previous study (Wang et al., 2021) to focus on the individual language performance prior to and independent of training and how it relates to the *individual* alpha power during task performance. We hypothesize that the difference in alpha power attenuation between language tasks of different complexity in task-relevant brain regions reflects the individual cognitive ability to handle the task, and hence might be associated with the observed performance. In particular, we examined the alpha power attenuation (at the individual peak frequency, determined at rest; see Methods) during the experimental task at different syntactic positions in the sentences, and the spatial localization on the cortex for the observed correlation effects.

2. Materials and methods

As we are reusing the data from our previous study, many of the methodological details are already described elsewhere (Wang et al., 2021). In the following, these aspects are presented as brief summary.

2.1. Participants

Thirty right-handed native German speakers (fifteen females) were enrolled in this study (mean age: 27, range from 20 to 34). Their reading span was 3.7 ± 0.9 (mean ± SD). No neurological diseases or hearing impairments were reported. Participants were naïve to the purposes of the experiment and gave their written informed consent prior to the experiment. The study was approved by the ethics committee of the University of Leipzig (471/16-EK).

2.2. Stimulus material

Two types of German sentences with single and double hierarchical center-embedding were auditorily presented (for examples, see Fig. S1). All sentences started with an introductory phrase followed by a relative clause initiated by a relative pronoun (e.g. dass / that). The beginning of each relative clause (brace) was labeled with *bxon* while the final verb of it was labeled with *bxoff* to identify the same level of embedding. The place holder x represents the embedding level. The resulting structures were [seon [b1on [b2on … b2off] b1off] seoff] for single embedding, and [seon [b1on [b2on [b3on … b3off] b2off] b1off] seoff] for double embedding sentences, where seon/seoff represent sentence onset and offset, respectively. See also Fig. S1 & S4.

2.3. Experimental procedures

The experiment included four sessions carried out on four working days within one week. The stimuli were presented by the software 'Presentation' (www.neurobs.com). On each day, participants listened to 33 sentences of each sentence type (i.e., single and double embedded), while MEG was measured. Across all four days, each participant received an individual randomization of all 264 sentences. None of the sentences was presented twice to the same participant. After each sentence, a content question was asked to test the understanding of the thematic role assignments (see Fig. S1 for examples). Each session comprised four blocks. Sentences were presented during the first three blocks. During the fourth block, resting-state MEG was recorded for at least 10 min. Participants were asked to close their eyes and stay awake.

2.4. Behavioral data analysis

Behavioral performance was measured through the accuracy of the participants' responses to the question task. In contrast to our previous study, the single valued total performance accuracy of each participant was estimated by a simple mean across the 4 experimental days.

2.5. MEG data acquisition and preprocessing

After preprocessing, the data of the first three blocks (task sections) were epoched of 0.5 s length starting with the event triggers at *b1on, b1off, b2on, b2off, b3on, and b3off* (on for embedding's begin, and off for embedding's closure). Data of the fourth block (rest section, total 12 min) were epoched into 36 trials of 20 s length each to get a frequency resolution of 0.05 Hz for the determination of the peak frequency. After artifact rejection, the median value of number of valid trials was 34, ranging from a minimum of 6 to a maximum of 35.

2.6. Estimation of individual spontaneous peak frequency in sensor space

The characteristics of the alpha peak (e.g., frequency and power) are specific for each individual (Furman et al., 2018; Grabot and Kayser, 2020; Gulbinaite et al., 2017; Horschig et al., 2014; Katyal et al., 2019; Migliorati et al., 2020; Minami et al., 2020; Sadaghiani and Kleinschmidt, 2016; Smit et al., 2006). Hence, the somewhat non-univocal picture regarding the relationship between individual alpha power dynamics and task performance might also be rooted in the insufficient capture of the individual oscillations by using the classical broad frequency band (about 8–12 Hz). We therefore decided to first determine the individual alpha frequency from the pre-processed resting state MEG, and base our further analysis on the power at that frequency.

For each subject on each day, the power spectrum density (PSD) for each sensor was estimated using the multi-taper method via the function *psd_multitaper* from the MNE-python v.0.16 (Gramfort et al., 2013) (using default setup, except normalization = 'full'). The PSDs for each 20s-length trial were transformed to logarithmic scale (i.e., in dB) and then averaged across trials and sensors. After averaging, the 1/f pink noise background was estimated and subtracted from each average PSD. To estimate the 1/f trend line in the PSD, the PSD was first cropped to the frequency range 1 Hz to 120 Hz, which was transformed to logarithmic scale (base 10). Then, the PSD were fed to a first-degree polynomial fit function (in Python: use *numpy.polyfit* to get the polynomial parameters and use *numpy.polyval* to recover the trend line). In order to eliminate the impact of the local peaks in the PSD onto the fitting, we used an interactive procedure (see Fig. S2). We first estimated the trend line, then removed the parts in the PSD above that trend line (Fig. S2C), and then estimated a new trend from the remaining data (Fig. S2D). We repeated this procedure, until the root mean square (RMS) difference between two subsequent trend lines was less than 0.005. The detrended PSDs for each participant and each training day are shown in Fig. S3. The global maxima within the band 7–29 Hz were identified as the individual peak frequency. Those participants with individual peak frequency higher than 13 Hz (thus in the beta range) were removed from further analysis. This resulted in the removal of 6 participants out of the 30 participants. The motivation for this strategy was that these very dominant beta peaks were also very wide, with their flanks overlapping with, and therefore potentially contaminating, the much smaller alpha peaks. Additional analyses using only the global maxima between 7 and 13 Hz and not excluding any subjects yielded equivalent significant results, albeit with generally lower correlation values.

2.7. Estimation of alpha power during the task in source space

For source localization, we used individual single shell volume conductor models and source models constructed from the individual T1-weighted MR data. We utilized Freesurfer 6.0.0 to segment the inner

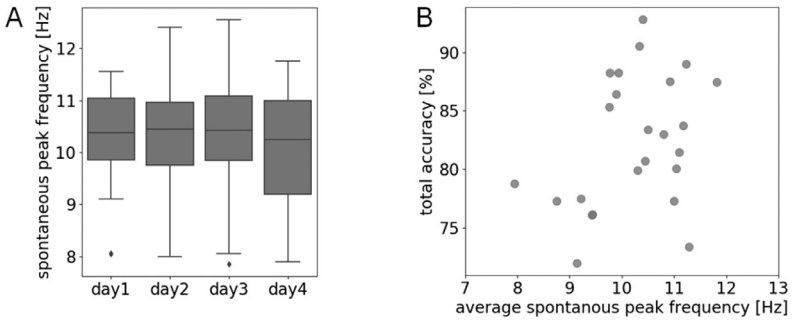

Fig. 1. Relationship between the individual spontaneous peak frequency and the language task performance. (A) Boxplot of the participants' individual spontaneous peak frequencies on each training day. The boxes show the interquartile ranges that stretch from the first quartile (25th percentile) to the third quartile (75th percentile) with the black line marking the median (50th percentile). The maximal whisker range is 1.5 times the interquartile range. Note that the displayed whisker length depends on values within whisker range. Diamonds represent outliers, that is, values outside the whisker range. (B) Scatter plot showing the correlation between the total performance accuracy and the spontaneous peak frequency, both averaged over experimental days.

skull as well as the cortical surface. Finally, the cortical surfaces were labeled according to Glasser et al. (2016). Based on the rationale that activity related to cognitive performance should be sensitive to task difficulty, we focus on those left temporal-parietal regions (A4, A5, PSL, STV, TPOJ1–3, PF, PFm, and PGi, labels according to Glasser et al., 2016), which in our previous analysis (Wang et al., 2021) had shown significant sentence complexity effects for the alpha power (see Fig. 3A).

To estimate the alpha power in source space, we used the LCMV beamformer method (Van Veen et al., 1997) via the function *make_lcmv* by MNE-python v.0.16. The reconstructed current density was restricted to being perpendicular to the cortical surface. The noise covariance matrix was computed as the mean noise covariance from the empty room measurements obtained before and after each recording session. A data covariance matrix was computed separately for each day based on the whole sentence data. The PSD (in dB) of each source was estimated using the multi-taper method (*psd_multitaper*, data zero-padding to 2 s), separately for each subject, ROI, sentence type, and day as mean over all presented sentences. The 1/f pink noise background was estimated and subtracted from each average PSD separately. To estimate the spectral power of the individual peak frequency at task, we averaged the spectral power of the two frequency bins, which define the interval around the individual peak frequency at rest. Finally, relative power attenuation was calculated by normalizing to the respective *b1on* power value separately for each subject, ROI, sentence type, and day. Hence, all subsequently reported spectral power values in task conditions are relative power attenuations with respect to *b1on*.

For computing the individual frequency power in Yeo's 17-networks (Yeo et al., 2011; Fig. 5A), we first morphed the individual source space to the fsaverage space via the source morph function in MNE-python v.0.16 (by setting fsaverage spacing „ico5"). The remaining steps were as same as for using the Glasser's ROIs.

3. Results

3.1. Individual resting-state peak frequency

The individual peak frequency was estimated from the resting-state recordings at sensor level (for more details, see Materials and Methods Section 2.6.). We first estimated it for each subject on each day and then averaged it across the four days. The overall task performance was calculated for each subject by averaging the accuracy scores of the four experimental days, including, both, double and single embedded sentences. We found no statistical difference among the estimated individual peak frequencies of the four experimental days (Friedman's test $Q = 0.49$, $p = 0.92$; Fig. 1A). We also found no significant association between the 4-day-average individual peak frequency and the total performance accuracy (Spearman's correlation, $r = 0.31$, $p = 0.14$; Fig. 1B).

Second, we examined the relationship between the power at the individual peak frequency during rest (average across four days) and the total performance accuracy. The power was also first estimated for each subject on each day and then averaged across the four days (Fig. 2C). There were no detectable power differences between the four experimental days (Friedman's test $Q = 23.50$, $p = 0.4839$; Fig. 2A). We found no clear association between the (average) power and the performance accuracy (Spearman's correlation, $r = 0.01$, $p = 0.96$; Fig. 2B).

3.2. Relationship between in-task alpha power and language performance

Average time-frequency representations as well as alpha power over the entire sentence length are shown for both sentence types in Fig. S4. Note that the sentences were of different lengths, and so were the distances between adjacent syntactic positions. Therefore, the individual time-frequency spectra had to be piecewise scaled prior to averaging.

We examined the power at the individual alpha peak frequencies (as determined during rest, see above) when participants were hearing the sentences, and tested its relationship with the language task performance at single subject level. We expected that the *difference* in power attenuation between the double embedded and single embedded sentences would reflect the subjects' ability to process the sentences. To test this hypothesis, we focused on the brain regions (Fig. 3A), for which our previous study (Wang et al., 2021) found a significant difference in the alpha power (8–12 Hz) attenuation between the double and single embedding conditions at the final closure of the embedding structure (*b1off*; for the meaning of the trigger point labels *b1on, b1off, b2on, b2off*, see Section 2.2 and Fig. S1 & S4). We first examined, whether by using the individual resting-state peak frequency, we can replicate our previous result obtained with the broad alpha band (sentence effect: general power attenuation difference between double and singled embedded sentences). In Fig. 3B we show the power decrease at the individual peak frequency at *b1off* (*b1off-b1on*) for each sentence type and each day. A non-parametric ANOVA (Wobbrock et al., 2011) for the factors sentence (double vs. single) and day (1 through 4) yielded only a significant main effect for the factor sentence ($F = 18.95$, $p < 0.00003$), which is in alignment with our previous report using broad-band alpha band 8–12 Hz (Wang et al., 2021). Averaged across all four days, for both types of sentences, the alpha power decreases when the sentence unfolds (see also Fig. S4). The difference between the power attenuation between sentence types increased over the sentence and was most pronounced at *b1off* (Fig. 3C). The power attenuations at *b1off* for single and double embedded sentences were strongly correlated (Spearman's correlation $r = 0.84$, $p < 0.0000004$; Fig. 3D).

Most importantly, as hypothesized, at *b1off*, the alpha power attenuation difference between single and double embedded sentences was correlated with the individual task performance (Spearman's correlation $r = -0.70$, $p = 0.0004$; Fig. 3E): participants who showed a larger power attenuation difference between the two sentence types at their individual peak frequency achieved better overall accuracy. Moreover, those participants, who showed a larger power attenuation for the double embedded sentences also performed better (Spearman's $r = -0.59$, $p = 0.016$ see Fig. 3E).

When using the classical frequency band (8–12 Hz, as used in (Wang et al., 2021)) instead of the individual peak frequency, the by-subject correlation between *b1off* power attenuation difference (double vs. single) and the performance reduced to $r = -0.50$ (Spearman's corre-

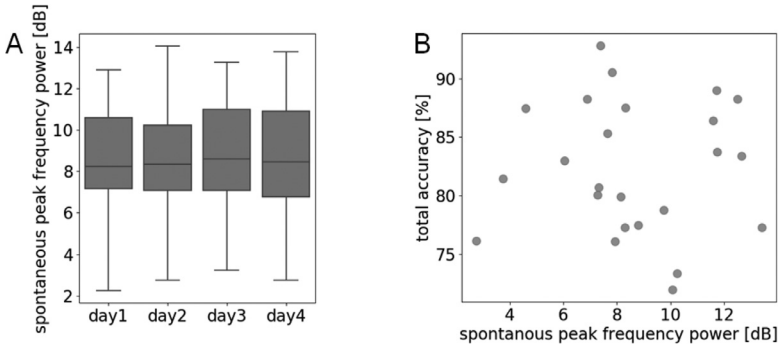

Fig. 2. Relationship between the power of individual spontaneous peak frequency during rest and language task performance. (A) Boxplot of participants' individual spontaneous peak frequency power for each training day (for details, refer to Fig. 1). (B) Scatter plot showing the correlation over participants between the total performance accuracy and the average spontaneous peak frequency power. Total performance accuracy was calculated by averaging the accuracy scores of the four experimental days, including, both, double and single embedded sentences.

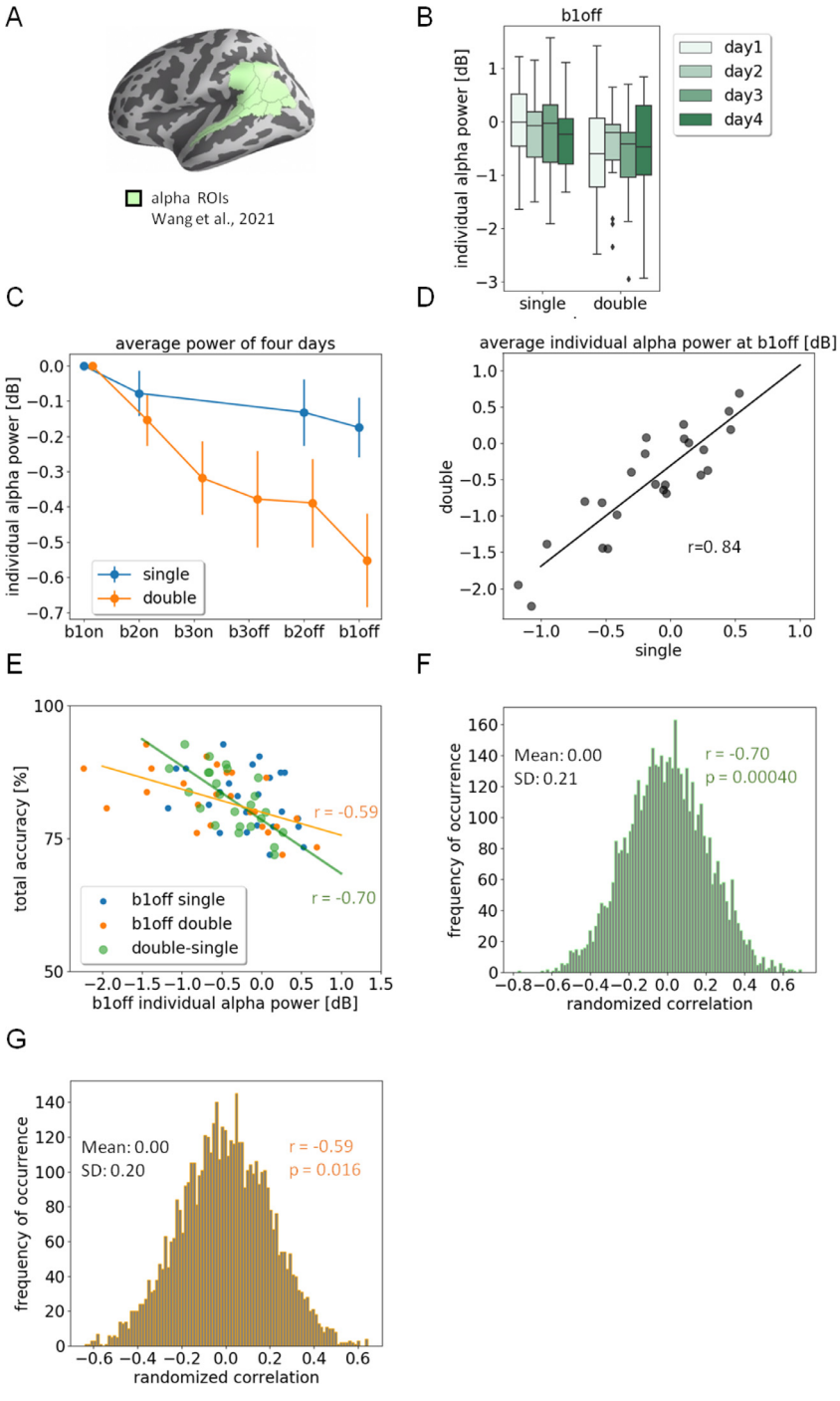

Fig. 3. Relationship between the power attenuation at individual peak frequency during task and the language task performance. (A) Pre-selected ROIs that were reported to show significant power attenuation difference between double- and single embeddings at the final closure of the embedded structure in Wang et al., 2021. (B) Boxplot of the individual alpha power attenuation for each sentence type and each day. The individual alpha power attenuation was estimated by the power of the individual peak frequency at the final closure of the embedded structure (*b1off*) minus the power at the start of the embedded structure (*b1on*). (C) Four-days-average individual alpha power attenuation for each sentence type at different openings and closures of the embedded structure. Points show the mean value of the thirty participants, vertical lines show the standard error. The power of *b1on* (opening of the embeddings) was used as baseline for the other positions. (D) The individual alpha power attenuations at the final closures (*b1off*) for double and single embedded sentences were strongly associated (Spearman's correlation, $p = 3.17 \cdot 10^{-7}$). (E) The power attenuation differences between double and single embedded sentences at the individual alpha frequency at the final closure were associated with the individual performance accuracy (Spearman's correlation $r = -0.70$); individual peak frequency power attenuation for double embedded sentences was associated with the performance accuracy (Spearman's $r = -0.59$). (F) Permutation-test of the association between the individual alpha power attenuation differences (double vs. single embedded sentence) at the final closure and the individual task performance. The power attenuations of the single as well as the double embedded sentences were permuted 5000 times. The mean of the randomized Spearman's correlation was 0.00 and the standard deviation was 0.21. The probability of appearance of a correlation value less than $r = -0.7$ was 0.0004. (G) Same as F for double embedded sentences (mean correlation 0.00, standard deviation 0.20, probability of $r < -0.59$ was 0.016).

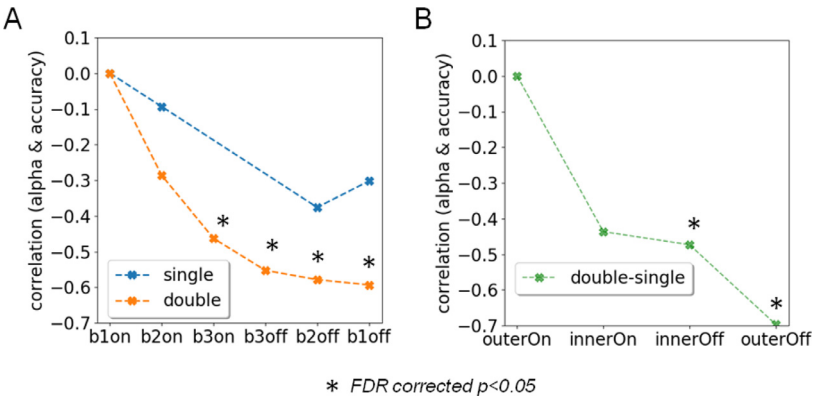

Fig. 4. Association of the individual peak frequency power attenuation and the language performance at different positions of embedded structures. (A) Spearmans' correlation between the individual peak frequency power attenuation (with respect to baseline b1on) for double and single embedded sentences and the total performance accuracy. (B) Spearmans's correlation between the individual peak frequency power attenuation difference (double-single) and the total performance accuracy at different syntactically equivalent position. Position labels: outerOn: b1on for single and double; innerOn: b2on for single and b3on for double; innerOff: b2off for single and b3off for double; outerOff: b1off for single and double.

lation, $p = 0.0049$), and the correlation between the *b1off* power attenuation for double embedding and the performance dropped to $r = -0.28$ (Spearman's correlation, $p = 0.13$; see Fig. S5).

3.3. Temporal exploration: association of alpha power attenuation and language performance at different embedding levels

Fig. 4A shows the Spearman's correlation between the total performance accuracy and the individual peak frequency power attenuation (i.e., with respect to *b1on*) for both sentence types at different positions of the embedded structure. Fig. 4B shows, at individual peak frequency, the power attenuation *difference* between the two sentence types at equivalent positions: *innerOn/innerOff* and *outerOn/outerOff* (opening/closure of the innermost/outermost embedded structures). After FDR-correction, we found several significant correlations along the processing of the double embedded sentences (Spearman's correlation, b3on: $r = -0.46$, b3off: $r = -0.55$, b2off: $r = -0.57$, b1off: $r = -0.59$, FDR $p<0.05$; Fig. 4A). In addition to the power attenuation difference at the final embedding closure, which were already reported (Fig. 3E), we found a performance correlation with the power attenuation difference at the first embedding closure (*innerOff*; Spearman's $r = -0.47$, FDR $p<0.05$; Fig. 4B).

3.4. Spatial exploration: association of alpha power attenuation and language performance at the functional network level

We explored the correlation between the individual peak frequency power attenuation and the power attenuation difference (double vs. single embedding) of the individual peak frequency at *b1off* and the total performance at the level of the entire cortex. In order to achieve maximum specificity to functional networks, we used the Yeo's 17-networks (Yeo et al., 2011) to define the brain ROIs (Fig. 5A). The power attenuation difference in the left as well as right temporal-parietal network (including the anterior and posterior superior temporal gyrus, Fig. 5A bright blue ROI) was significantly correlated with task performance (Spearman's $r = -0.62$ for left side and Spearman's $r = -0.61$ for right side, FDR corrected $p<0.05$; Fig. 5B&C). Also, we found the power attenuation for double embedded sentence in the left and right temporal-parietal network as well as some adjacent networks (in particular in the right hemisphere: default networks A&B and control network B) was significantly correlated with the performance (FDR corrected $p<0.05$; Fig. 5D).

Additional information about the spatial exploration of the correlation between the individual peak frequency power attenuation at the final closure of the embedded structure and the language performance based on the Glasser atlas (Glasser et al., 2016) can be found in Fig. 6. We obtained similar results as for the Yeo's 17-networks: in the left anterior and posterior superior temporal gyri, the power attenuation difference between double and single embedded sentences was correlated with the language performance, while for the right hemisphere, we found a significant effect in the middle superior temporal gyri. Moreover, we found that in the right middle and posterior superior temporal as well as inferior frontal gyri, the power attenuation for double embedded sentences was correlated with the performance. This is also in agreement with the results obtained from the Yeo's 17-networks: in the right hemisphere, the default networks A&B and control network B, which are related to the several regions in the temporal, parietal, and frontal lobes, were associated with the power attenuation for double embedded sentences (Fig. 5D).

4. Discussion

In this study, we investigated the association between individual language comprehension performance and alpha power under resting-state and in-task conditions. At rest, we did not find any significant changes over the course of the experiment nor any correlation with language performance for alpha power or individual alpha peak frequency.

Next, we turned to the MEG data acquired during task, by studying the alpha power attenuation (at the individual peak frequency determined at rest). We tested our hypothesis that the individual power attenuation over the course of each sentence predicts the individual language comprehension performance. As candidate areas, we first used those left-hemispheric temporo-parietal regions that already showed a group effect of sentence complexity in the alpha band (Wang et al., 2021). Indeed, we found correlations for, both, the power attenuation observed for the more complex sentences (double embedding) and the difference in power attenuation between the two complexity levels.

Interestingly, the subsequent whole-brain spatial analysis, using either Yeo's 17-networks or Glasser's atlas, confirms that performance correlations with the difference between the power attenuations are present in a superior temporal and inferior parietal network that is very similar to the one reported in Wang et al. (2021). However, it turns out that not only the left hemispheric network, but also the right hemispheric homologue show this correlation.

Moreover, the whole brain analysis also revealed that for the double embedded sentences, the performance correlated with the alpha power attenuation in the left hemisphere for similar regions as for the double-single power attenuation difference, but in the right hemisphere for more extended temporal, parietal, and even frontal areas (see especially Fig. 6).

In summary, the following observations underscore the functional role of alpha oscillations in language processing: (i) individual performance was correlated with alpha power attenuation during task but not with alpha power at rest, and (ii) these effects were localized in left temporal-parietal brain regions usually associated with language processing and, even more pronounced, in their right hemisphere homologues.

Cortical alpha activity has been proposed to play an important role in excitability regulation mechanisms underlying various human cognitive

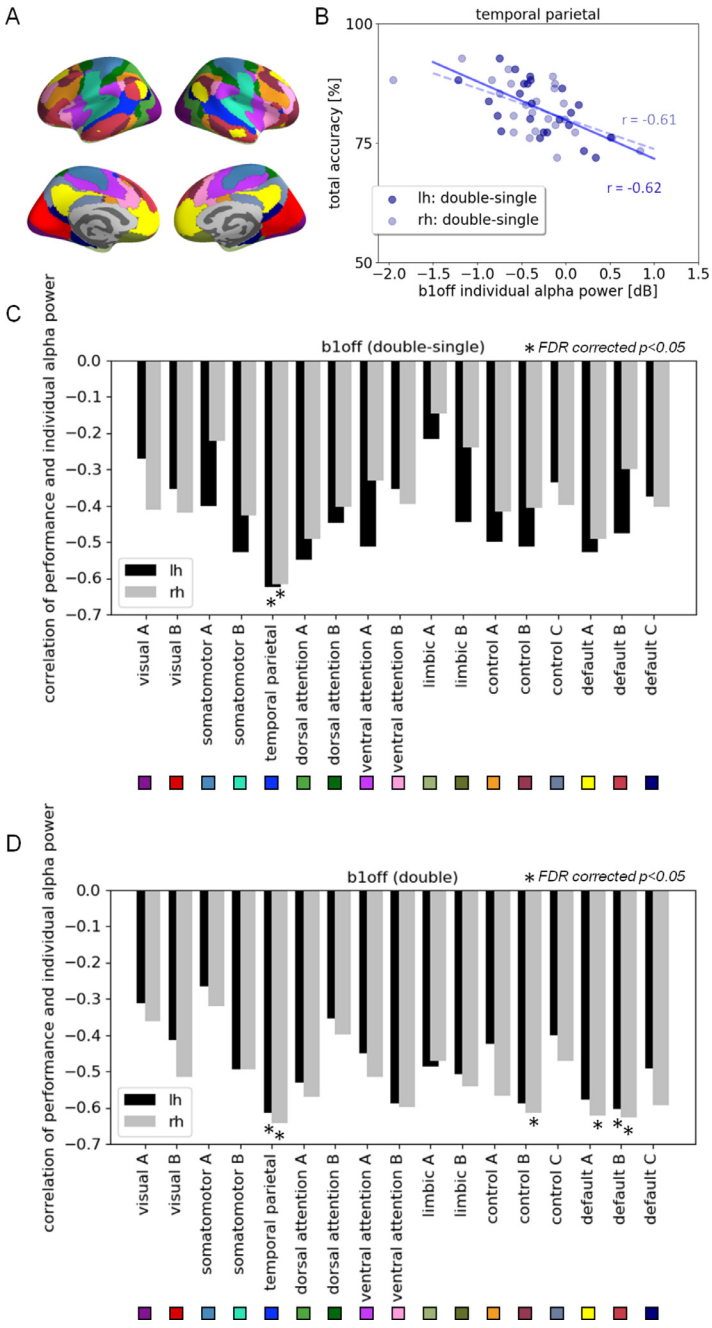

Fig. 5. Association of the individual peak frequency power attenuation and the language performance at the functional networks level. (A) ROIs of Yeo's 17-networks. The temporal parietal network is painted in bright blue. (B) Individual peak frequency power attenuation difference (double-single embeddings) at the final closure of the embedded structures (b1off) in the left and right temporal-parietal network was significantly associated with the performance (Spearmans' $r = -0.62$ and $r = -0.61$, FDR corrected $p<0.05$). (C)&(D) Spatial distribution of Spearman's correlation between individual peak frequency power attenuation difference (double-single embeddings; C) as well as power attenuation of double (D) at the final closure of the embedded structures (*b1off*) and the individual performance accuracy on Yeo's 17-networks.

abilities, including memory, attention, perception, etc. Task irrelevant regions exhibit higher alpha power reflecting inhibition, while in task relevant regions alpha power is reduced, reflecting increased excitability (Foxe and Snyder, 2011; Jensen and Mazaheri, 2010; Klimesch, 2012; Klimesch et al., 2007).

At rest, such an increased excitability could reflect a general predisposition of a person towards cognitive performance. In contrast, if observed during task within specific task relevant brain areas, it would index processes related to the particular task or experimental situation. Alpha power at rest has been found to be positively correlated with task performance in cognitive control (Mahjoory et al., 2019) and episodic memory (Sargent et al., 2021) tasks, but negatively correlated with language skills (Kwok et al., 2019). This somewhat non-univocal picture suggests that for different experimental situations, different levels of pre-inhibition and disinhibition of cortical areas are beneficial. On the other hand, during the actual task and within the task relevant areas, we would expect a clear attenuation of alpha, which scales with the actual engagement with the task, as reflected by task performance. There are a number of previous studies showing general alpha attenuation during task within task relevant areas (Hilla et al., 2020; Magosso et al., 2019; Wang et al., 2021). These works show that the alpha oscillation power is related to the specific task demand. This is reflected in our results by the finding that the individual alpha power attenuation is stronger for the more complex sentences and increases with increasing cognitive (including working memory) load along the sentence (Fig. 4). On the other hand, evidence for a correlation between alpha power modulation in specific task-relevant brain areas and individual task performance is scarce. By clearly demonstrating this in our study, we show that in-task alpha power attenuation actually reflects processes that are involved in successful task completion. This is further corroborated by the fact that

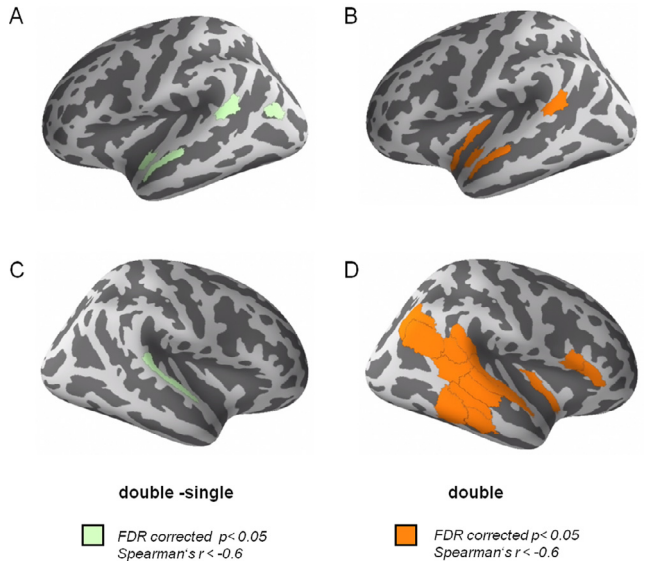

Fig. 6. Association of the peak frequency power attenuation and the language performance with the Glasser atlas. Spearman's correlations were calculated between the total performance accuracy and the (i) power attenuation difference (double vs. single embeddings) at the final closure of the embedded structure (b1off) as well as the power attenuation at the final closure for (ii) double and (iii) single embedded sentences for 360 ROIs. FDR-correction was based on all 1080 tests. Significant level is $p<0.05$. Significant regions are highlighted (there were none for single embedded sentences). (A) & (C) ROIs that showed the association between power attenuation difference (double vs. single embeddings) and the total performance accuracy. (B) & (D) ROIs that showed the association between power attenuation for double embedded sentences and the total performance accuracy.

also the correlation between alpha power and task performance seems to build up over the course of the sentence and therefore increase with cognitive load (Section 3.3).

Along with the idea that the association of the alpha power and performance may indicate the task engagement of the brain regions, our whole brain results based on Yeo's 17-networks suggest that the temporal-parietal network plays a crucial role in processing the embedding. We further cross-checked and refined this by exploring the association using the whole 360 ROI brain parcellation from the Glasser atlas and found a particularly high association between power attenuation difference (double vs. single) and performance in the superior temporal gyrus (Fig. 6). This is in alignment with the literature showing that the posterior superior temporal gyrus plays an important role in processing embedded structures (Friederici, 2011; Friederici et al., 2006; Kinno et al., 2008; Röder et al., 2002). Regarding the findings in the two homologue networks in the left and right hemispheres, we infer that even though the areas in the left hemisphere may form the classical language network (Friederici, 2011; Hickok and Poeppel, 2004; Poeppel et al., 2012; Vigneau et al., 2006), homologue areas in the right hemisphere may increasingly engage when task demands are high as a result of enhanced working memory loads (Fridriksson and Morrow, 2005). Moreover, it has been shown that increased difficulty in language learning tasks leads to increased involvement of right hemisphere areas (Chen et al., 2021; Qi et al., 2019). This would explain why we find such widespread right hemispheric effects specifically for the double embedded sentences. However, why did we not find a similar asymmetry for the double-single difference and no significant results for the single condition? We may assume that the performance correlation of the alpha power does exist in both complexity conditions, but is much weaker for the single embedding sentences, such that it escapes detectability in the current data. Assuming that the main sources of variance are random (i.e., not correlated between complexity conditions), the correlation for the difference double-single must be weaker than that for the double condition alone. Therefore, it may only be detected in areas with stronger attenuation. These might be the core language areas shown in Fig. 6A,C and Fig. 5A (blue network). For the double condition, we have the strongest correlation, which is also seen in additional areas, especially in the right hemisphere.

5. Conclusion

In summary, in this present paper, we used a language comprehension experiment to demonstrate that by manipulation of the task complexity, the alpha power attenuation in the task relevant brain regions reflects the increase of the cognitive load and predicts the individual performance outcome. Individual alpha power could be a useful biomarker to highlight the relevant brain regions and monitor the brain states during the cognitive processing.

Data availability statement

Anonymized raw data will be made available upon request via email to the corresponding author provided the requesting researchers sign a formal data sharing agreement and cite this paper as origin of the data.

Credit authorship contribution statement

P. Wang: Conceptualization, Methodology, Software, Validation, Formal analysis, Data curation, Writing – original draft, Writing – review & editing, Visualization, Project administration. **Y. He:** Conceptualization, Methodology, Validation, Writing – review & editing. **B. Maess:** Investigation, Resources, Data curation, Writing – review & editing, Supervision, Project administration. **J. Yue:** Conceptualization, Methodology, Writing – review & editing. **L. Chen:** Writing – review & editing. **J. Brauer:** Investigation, Resources, Writing – review & editing. **A.D. Friederici:** Writing – review & editing, Funding acquisition. **T.R. Knösche:** Investigation, Resources, Writing – review & editing, Supervision, Project administration, Funding acquisition.

Acknowledgements

We like to thank Yvonne Wolff for carefully conducting the MEG experiments. This work was supported by the Deutsche Forschungsgemeinschaft, Grants KN588/7–1 and FR519/22–1 within SPP2041.

Supplementary materials

Supplementary material associated with this article can be found, in the online version, at doi:10.1016/j.neuroimage.2022.119449.

References

Berger, H., 1938. Über das Elektroenkephalogramm des Menschen. XIV. Arch. Psychiatr. Nervenkr..

Chen, L., Wu, J., Hartwigsen, G., Li, Z., Wang, P., Feng, L., 2021. The role of a critical left fronto-temporal network with its right-hemispheric homologue in syntactic learning based on word category information. J. Neurolinguistics 58, 100977.

Foxe, J.J., Snyder, A.C., 2011. The role of alpha-band brain oscillations as a sensory suppression mechanism during selective attention. Front. Psychol. 2, 1–13. doi:10.3389/fpsyg.2011.00154.

Fridriksson, J., Morrow, L., 2005. Cortical activation and language task difficulty in aphasia. Aphasiology 19, 239–250.

Friederici, A.D., 2011. The brain basis of language processing: from structure to function. Physiol. Rev. 91, 1357–1392.

Friederici, A.D., Bahlmann, J., Heim, S., Schubotz, R.I., Anwander, A., 2006. The brain differentiates human and non-human grammars: functional localization and structural connectivity. Proc. Natl. Acad. Sci. U. S. A. 103, 2458–2463. doi:10.1073/pnas.0509389103.

Furman, A.J., Meeker, T.J., Rietschel, J.C., Yoo, S., Muthulingam, J., Prokhorenko, M., Keaser, M.L., Goodman, R.N., Mazaheri, A., Seminowicz, D.A., 2018. Cerebral peak alpha frequency predicts individual differences in pain sensitivity. Neuroimage 167, 203–210.

Gastaldon, S., Arcara, G., Navarrete, E., Peressotti, F., 2020. Commonalities in alpha and beta neural desynchronizations during prediction in language comprehension and production. Cortex 133, 328–345. doi:10.1016/j.cortex.2020.09.026.

Glasser, M.F., Coalson, T.S., Robinson, E.C., Hacker, C.D., Harwell, J., Yacoub, E., Ugurbil, K., Andersson, J., Beckmann, C.F., Jenkinson, M., 2016. A multi-modal parcellation of human cerebral cortex. Nature 536, 171–178.

Grabot, L., Kayser, C., 2020. Alpha activity reflects the magnitude of an individual bias in human perception. J. Neurosci. 40, 3443–3454.

Gramfort, A., Luessi, M., Larson, E., Engemann, D.A., Strohmeier, D., Brodbeck, C., Goj, R., Jas, M., Brooks, T., Parkkonen, L., 2013. MEG and EEG data analysis with MNE-Python. Front. Neurosci. 7, 267.

Gulbinaite, R., van Viegen, T., Wieling, M., Cohen, M.X., VanRullen, R., 2017. Individual alpha peak frequency predicts 10Hz flicker effects on selective attention. J. Neurosci. 37, 10173–10184.

Hickok, G., Poeppel, D., 2004. Dorsal and ventral streams: a framework for understanding aspects of the functional anatomy of language. Cognition 92, 67–99.

Hilla, Y., von Mankowski, J., Föcker, J., Sauseng, P., 2020. Faster Visual Information Processing in Video Gamers Is Associated With EEG Alpha Amplitude Modulation. Front. Psychol. 11, 3333.

Horschig, J.M., Jensen, O., van Schouwenburg, M.R., Cools, R., Bonnefond, M., 2014. Alpha activity reflects individual abilities to adapt to the environment. Neuroimage 89, 235–243.

Jensen, O., Mazaheri, A., 2010. Shaping functional architecture by oscillatory alpha activity: gating by inhibition. Front. Hum. Neurosci. 4, 186.

Jones, S.R., Kerr, C.E., Wan, Q., Pritchett, D.L., Hämäläinen, M., Moore, C.I., 2010. Cued spatial attention drives functionally relevant modulation of the mu rhythm in primary somatosensory cortex. J. Neurosci. 30, 13760–13765.

Katyal, S., He, S., He, B., Engel, S.A., 2019. Frequency of alpha oscillation predicts individual differences in perceptual stability during binocular rivalry. Hum. Brain Mapp. 40, 2422–2433.

Kinno, R., Kawamura, M., Shioda, S., Sakai, K.L., 2008. Neural correlates of noncanonical syntactic processing revealed by a picture-sentence matching task. Hum. Brain Mapp 29, 1015–1027.

Klimesch, W., 2012. Alpha-band oscillations, attention, and controlled access to stored information. Trends Cogn. Sci. 16, 606–617. doi:10.1016/j.tics.2012.10.007.

Klimesch, W., Pfurtscheller, G., Mohl, W., Schimke, H., 1990. Event-related desynchronization, ERD-mapping and hemispheric differences for words and numbers. Int. J. Psychophysiol. 8, 297–308.

Klimesch, W., Sauseng, P., Hanslmayr, S., 2007. EEG alpha oscillations: the inhibition—timing hypothesis. Brain Res. Rev. 53, 63–88.

Kuhnke, P., Meyer, L., Friederici, A.D., Hartwigsen, G., 2017. Left posterior inferior frontal gyrus is causally involved in reordering during sentence processing. Neuroimage 148. doi:10.1016/j.neuroimage.2017.01.013.

Kwok, E.Y.L., Cardy, J.O., Allman, B.L., Allen, P., Herrmann, B., 2019. Dynamics of spontaneous alpha activity correlate with language ability in young children. Behav. Brain Res. 359, 56–65. doi:10.1016/j.bbr.2018.10.024.

Magosso, E., De Crescenzio, F., Ricci, G., Piastra, S., Ursino, M., 2019. EEG alpha power is modulated by attentional changes during cognitive tasks and virtual reality immersion. Comput. Intell. Neurosci. 2019. doi:10.1155/2019/7051079.

Mahjoory, K., Cesnaite, E., Hohlefeld, F.U., Villringer, A., Nikulin, V.V., 2019. Power and temporal dynamics of alpha oscillations at rest differentiate cognitive performance involving sustained and phasic cognitive control. Neuroimage 188, 135–144.

Mann, C.A., Sterman, M.B., Kaiser, D.A., 1996. Suppression of EEG rhythmic frequencies during somato-motor and visuo-motor behavior. Int. J. Psychophysiol. 23, 1–7.

Meyer, L., 2018. The neural oscillations of speech processing and language comprehension: state of the art and emerging mechanisms. Eur. J. Neurosci. doi:10.1111/ejn.13748.

Meyer, L., Obleser, J., Friederici, A.D., 2013. Left parietal alpha enhancement during working memory-intensive sentence processing. Cortex 49, 711–721.

Migliorati, D., Zappasodi, F., Perrucci, M.G., Donno, B., Northoff, G., Romei, V., Costantini, M., 2020. Individual alpha frequency predicts perceived visuotactile simultaneity. J. Cogn. Neurosci. 32, 1–11.

Minami, S., Oishi, H., Takemura, H., Amano, K., 2020. Inter-individual differences in occipital alpha oscillations correlate with white matter tissue properties of the optic radiation. eNeuro 7.

Pfurtscheller, G., 2003. Induced Oscillations in the Alpha Band: functional Meaning. Epilepsia 44, 2–8. doi:10.1111/j.0013-9580.2003.12001.x.

Pfurtscheller, G., 1989. Functional Topography During Sensorimotor Activation Studied with Event-Related Desynchronization Mapping. J. Clin. Neurophysiol. 6, 75–84. doi:10.1097/00004691-198901000-00003.

Poeppel, D., Emmorey, K., Hickok, G., Pylkkänen, L., 2012. Towards a new neurobiology of language. J. Neurosci. 32, 14125–14131.

Qi, Z., Han, M., Wang, Y., de Los Angeles, C., Liu, Q., Garel, K., San Chen, E., Whitfield–Gabrieli, S., Gabrieli, J.D.E., Perrachione, T.K., 2019. Speech processing and plasticity in the right hemisphere predict variation in adult foreign language learning. Neuroimage 192, 76–87.

Röder, B., Stock, O., Neville, H., Bien, S., Rösler, F., 2002. Brain activation modulated by the comprehension of normal and pseudo-word sentences of different processing demands: a functional magnetic resonance imaging study. Neuroimage 15, 1003–1014.

Sadaghiani, S., Kleinschmidt, A., 2016. Brain networks and α-oscillations: structural and functional foundations of cognitive control. Trends Cogn. Sci. 20, 805–817.

Sargent, K., Chavez-Baldini, U., Master, S.L., Verweij, K.J.H., Lok, A., Sutterland, A.L., Vulink, N.C., Denys, D., Smit, D.J.A., Nieman, D.H., 2021. Resting-state brain oscillations predict cognitive function in psychiatric disorders: a transdiagnostic machine learning approach. NeuroImage Clin 30, 102617.

Schomer, D.L., Da Silva, F.L., 2012. Niedermeyer's electroencephalography: Basic principles, Clinical applications, and Related Fields. Lippincott Williams & Wilkins.

Smit, C.M., Wright, M.J., Hansell, N.K., Geffen, G.M., Martin, N.G., 2006. Genetic variation of individual alpha frequency (IAF) and alpha power in a large adolescent twin sample. Int. J. Psychophysiol. 61, 235–243.

Yeo, B.T., Krienen, F.M., Sepulcre, J., Sabuncu, M.R., Lashkari, D., Hollinshead, M., Roffman, J.L., Smoller, J.W., Zöllei, L., Polimeni, J.R., 2011. The organization of the human cerebral cortex estimated by intrinsic functional connectivity. J. Neurophysiol. 106, 1125–1165.

Van Dijk, H., Schoffelen, J.-.M., Oostenveld, R., Jensen, O., 2008. Prestimulus oscillatory activity in the alpha band predicts visual discrimination ability. J. Neurosci. 28, 1816–1823.

van Ede, F., Köster, M., Maris, E., 2012. Beyond establishing involvement: quantifying the contribution of anticipatory α-and β-band suppression to perceptual improvement with attention. J. Neurophysiol. 108, 2352–2362.

Van Schijndel, M., Murphy, B., Schuler, W., 2015. Evidence of syntactic working memory usage in MEG data. In: Proceedings of the 6th Workshop on Cognitive Modeling and Computational Linguistics, pp. 79–88.

Van Veen, B.D., Van Drongelen, W., Yuchtman, M., Suzuki, A., 1997. Localization of brain electrical activity via linearly constrained minimum variance spatial filtering. IEEE Trans. Biomed. Eng. 44, 867–880.

Vassileiou, B., Meyer, L., Beese, C., Friederici, A.D., 2018. Alignment of alpha-band desynchronization with syntactic structure predicts successful sentence comprehension. Neuroimage 175. doi:10.1016/j.neuroimage.2018.04.008.

Vigneau, M., Beaucousin, V., Hervé, P.-.Y., Duffau, H., Crivello, F., Houde, O., Mazoyer, B., Tzourio-Mazoyer, N., 2006. Meta-analyzing left hemisphere language areas: phonology, semantics, and sentence processing. Neuroimage 30, 1414–1432.

Wang, P., Knösche, T.R., Chen, L., Brauer, J., Friederici, A.D., Maess, B., 2021. Functional brain plasticity during L1 training on complex sentences: changes in gamma-band oscillatory activity. Hum. Brain Mapp. 1–13. doi:10.1002/hbm.25470.

Wobbrock, J.O., Findlater, L., Gergle, D., Higgins, J.J., 2011. The aligned rank transform for nonparametric factorial analyses using only anova procedures. In: Proceedings of the SIGCHI Conference on Human Factors in Computing Systems, pp. 143–146.